TECHNICAL TRANSACTIONS | **CZASOPISMO TECHNICZNE**
ELECTRICAL ENGINEERING | ELEKTROTECHNIKA
2-E/2016

DOI: 10.4467/2353737XCT.16.253.6052

MIECZYSŁAW ZAJĄC*, MACIEJ SUŁOWICZ**

THE DETECTION OF COIL SHORTING IN INDUCTION MOTORS BY MEANS OF WAVELET ANALYSIS

ANALIZA FALKOWA W ZASTOSOWANIU DO WYKRYWANIA STANÓW ZWARĆ MIĘDZYZWOJOWYCH SILNIKA INDUKCYJNEGO

Abstract

This paper presents the results of an analysis of signals recorded in different inter-turn short- circuit states in the stator windings of a squirrel-cage motor operating under a constant load. The analysis was carried out in a time-frequency domain using a simple orthonormal wavelet base that can be used in a real system without the need to acquire specialist software. The choice of analytical was associated with the existence of a periodic energy flow between adjacent frequency bands, thus making it difficult to diagnose the Fourier analysis. The aim of the study was to gather data necessary for the development of a real-time diagnostic system. Magnetic axial flux, the zero voltage signal, the short-circuit current, vibration acceleration, sound pressure, electromechanical torque, currents and phase voltages were tested as diagnostic criteria. The paper presents the main results of the analyses of magnetic axial flux signal and conclusions.

Keywords: diagnostics of electromechanical systems, induction motor, short circuits, signal analysis, wavelet analysis

Streszczenie

W artykule przedstawiono wyniki analiz sygnałów zarejestrowanych w różnych stanach zwarć międzyzwojowych w uzwojeniach stojana silnika indukcyjnego pracującego pod stałym obciążeniem. Analizy przeprowadzono w domenie czasowo-częstotliwościowej, wykorzystując proste ortonormalne bazy falkowe, które można zastosować w układzie rzeczywistym bez potrzeby użycia specjalistycznego oprogramowania. Wybór metody badań był związany z istnieniem okresowych przepływów energii pomiędzy sąsiednimi pasmami częstotliwości, co utrudnia diagnozowanie przy wykorzystaniu analiz Fouriera. Celem przeprowadzonych badań było przyszłe wykorzystanie ich wyników do budowy działającego w czasie rzeczywistym systemu diagnostycznego. Jako sygnały diagnostyczne, których analiza pozwoli na sformułowanie diagnozy co do przyczyn asymetrii zasilania przetestowano m.in. sygnały proporcjonalne do strumienia poosiowego, napięcia zerowego, prądu w zwartych zwojach, przyspieszenia drgań, ciśnienia akustycznego, momentu elektromechanicznego oraz prądów i napięć fazowych. W artykule przedstawiono wyniki analiz sygnału proporcjonalnego do strumienia poosiowego oraz sformułowano wnioski.

Słowa kluczowe: diagnostyka układów elektromechanicznych, silnik indukcyjny, zwarcia międzyzwojowe, analiza sygnałów, analiza falkowa

* D.Sc. Ph.D. Eng. Mieczysław Zając, Assoc. Prof., Department of Automatic Control and Information Technology, Faculty of Electrical and Computer Engineering, Cracow University of Technology.

** Ph.D. Eng. Maciej Sułowicz, Institute of Electromechanical Energy Conversion, Faculty of Electrical and Computer Engineering, Cracow University of Technology.

Notations

$a(i, k, j)$ – signal wavelet approximation, i – signal number, k – representation level, j – consecutive number of signal sample in level support $k = N$,

$d(i, k, j)$ – signal wavelet detail, i – signal number, k – representation level, j – consecutive number of signal sample in level support $k = N$

$wf(i, k, l)$ – wavelet coefficient, i – signal number, k – representation level, l – consecutive number of wavelet coefficients in the support at the level k,

$E_d[i, fault, k]$ – wavelet detail energy, where i is the signal number, *fault* – type of fault, k – representation level.

1. Introduction

The subject of the research is the diagnosis of faults in an electromechanical system with a squirrel-cage induction motor operating under a constant load. During the research, the focus was on the diagnosis of faults in stator windings, which result in the asymmetry of electrical and magnetic circuits of a machine. This subject has been widely discussed in specialist literature, and initially, the basis for the discussion was classical methods of circuit analyses [11], such as the method of symmetrical components, which required significant simplification [2, 3, 13] – field methods were also applied. Later, several methods for the examination of signals were used, including methods in the time and frequency domain [4, 9, 10] sometimes together with computation intelligence methods [6–8, 12].

The results of tests performed on a real object were used in this paper. Time and frequency analysis of selected signals, which could carry information about the phenomena occurring during various short circuits in stator windings, was also performed. Cases of short circuits, defined by the number of short-circuited turns, were analysed, especially short circuits of two, three, four and five turns and the entire coil. The courses of signals proportional to the axial flux, a zero voltage level in the system of symmetrical components, short circuit current, sound pressure, electromechanical torque, acceleration vibration, as well as currents and phase voltages were used as the diagnostic criteria in this investigation. After the initial analysis of energy carried by each element of the distribution at each level of wavelet representation, the analysis became focused mainly on the use of signal wavelet representation proportional to the value of magnetic axial flux flowing along the machine shaft. This signal was used in diagnostics by many authors, for example, the authors of [1].

2. Laboratory measuring system

The object of the research was a squirrel-cage induction motor type Sg-112M-4 with parameters: $P_N = 4.0$ kW; $U_N = 380$ V; $I_N = 8.6$ A; $n_N = 1435$ rpm. The motor was mechanically connected by means of a clutch with a DC generator PZM5545 with the following specifications, which constitutes the mechanical load of the examined motor: $P_N = 4.5$ kW; $U_N = 230$ V; $I_N = 19.6$ A; $n_N = 1450$ rpm; $I_W = 0.86$ A.

In order to work out an effective algorithm of fault detections in motor windings at an early stage of fault appearance, the stator windings were deliberately modified. Selected winding turns from selected coils of stator windings were routed onto the machine casing. Turns from windings 1, 2, 3, 4, 5, 10, 15, 20, 25 and 51 were routed out. Owing to the fact that the turns were routed out, the simulation of short circuits of the selected number of stator windings was possible.

Fig. 1 shows the diagram of one coil of stator windings with the routed-out turns. The number at each turn indicates the number of the winding, which the turn was routed out from to the terminal box on the machine casing. Selected windings were short-circuited by connecting the appropriate numbers of routed-out turns with resistance and ammeter used to control the current in the short-circuited winding. An additional resistance was added in order to reduce current and to protect of the motor from overheating in the long-term measurements. The value of the additional resistance is about 5–6 Ohm and does not affect the effects originating from faults which are visible in the various details of the analyzed signals. Stator windings of the examined motor were joined in a star connection and powered from a low-voltage three-phase network.

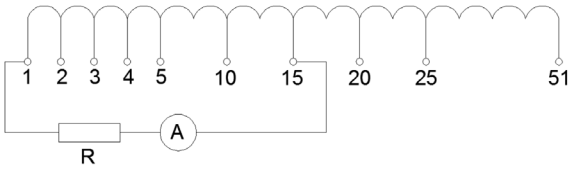

Fig. 1. Diagram of routed-out turns from one of the modified coils of stator windings

Apart from the modified motor windings, the coil for measuring axial flux installed on the bearing disc of the examined motor from the non-drive side is one of the most important elements of the measuring test bench. The view of the bearing disc with the measurement coil installed is shown in Fig. 2. The measurement coil was rolled up onto the resotex carcass with a diameter of around 90 mm. The coil is made from an enamel-insulated wire with a diameter of 0.25 mm; this coil contains around 2 200 turns.

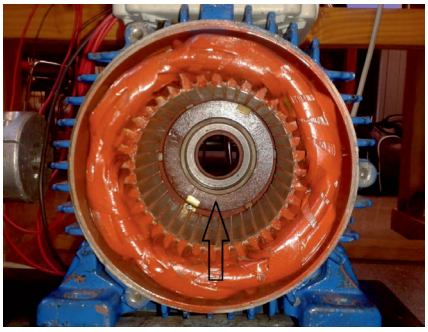

Fig. 2. View of the examined motor stator with the installed coil for measuring the axial flux

On Fig. 3 is shown schematic diagram of connections of all elements used during tests.

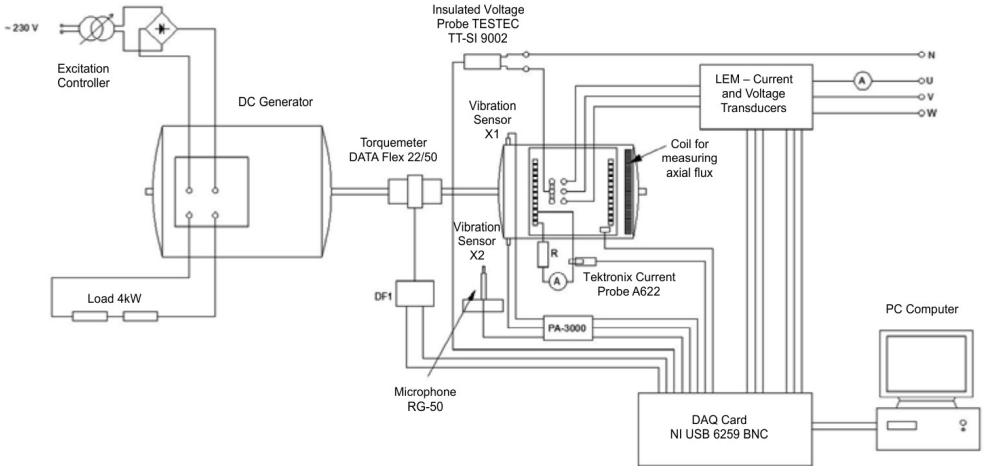

Fig. 3. Schematic diagram of connections of all elements used during tests

An adjustment system of a DC generator with an autotransformer and bridge rectifier was used during tests for changing the load of the examined motor. The load of the DC generator was created using two resistant heaters with a total power of 4 kW.

The load torque was measured with the torquemeter Data FLEX 22/50. A voltage signal proportional to rotational speed in the output of the torque-measuring device was also available.

For the measurement of phase currents and voltages, hall effect sensor transducers LEM were used. For the measurement of currents, three transducers HY 15 were used, and for the measurement of voltage, three transducers LV 25P were used. For measuring zero voltage between the connection point of the stator windings and the neutral point of the supply network, an insulated voltage probe TESTEC TT-SI 9002 was used. In addition, the current in the short-circuited windings was recorded. Current probe A622 Tektronix was used to perform the measurements.

Signals of vibration accelerations from two accelerometers ICP 603C01 installed on axis X on two opposite sides of the bearing disc were also recorded. The sound pressure signal was also recorded from a distance of about 60 cm from the examined motor. It was recorded with microphone RG-50. Signals from the accelerometers and the microphone were connected to signal conditioner PA-3000, and then from the conditioner to the measuring card NI USB 6259.

Apart from those three signals, signals from earlier listed measuring transducers were connected to the measuring card. Altogether, there were 14 signals sent to the measuring card. These were:

– three phase currents from transducers LEM HY 15;
– three phase voltages from transducers LEM LV 25P;
– electromagnetic torque;

– signal proportional to rotational speed;
– signal proportional to magnetic axial flux;
– current in the short-circuited winding;
– two signals of vibration acceleration in axis X on both sides of bearing disc;
– sound pressure;
– zero voltage.

All signals were recorded simultaneously with the use of measuring DAQ card NI 6259 and the dedicated software prepared MATLAB environment. Signals were sampled with a frequency of 50 kHz and the recording time for each measurement was 10 seconds. Data recording was performed for various levels of the simulated fault and various loads of the examined motor. All recorded data was then thoroughly analysed to determine which signals allow for efficient recognition of the smallest number of short-circuited turns windings – this is the most difficult task in the detection of these types of faults.

3. Calculation of elements of multiresolution wavelet decomposition for time series of the measuring data

The starting point of time and frequency analysis is the time series of the courses of the given variables recorded in the laboratory measuring system as signal samples $s(i, j)$, where i is the signal number, and j is the consecutive sample number in discrete time; therefore, $j = 1, \ldots, 500\,000$. The number of levels of wavelet representation is designated as N. It was decided that the full range of sampling frequency would be used, following the assumption that for the lowest scale levels (high frequencies), some details may be inappropriately recorded due to them arising as a result of faults.

For the first level, $k = 1$, the wavelet approximations $a(i, k, j)$ were calculated by making the signal vales for each pair of the signal's two consecutive samples average. At the next levels, $1 < k \leq N$, characterised by lower frequencies, a recursive procedure was applied. Wavelet approximations for level k were calculated by making the values of consecutive approximation pairs from level $k - 1$ average. Values of approximations calculated in such a manner were used to calculate wavelet details and also to calculate scale coefficients at consecutive levels of multiresolution representation. For each level, $k < N$, the approximation value in the selected time interval is the product of the appropriate scale coefficient and normalised value of a scaling function shifted in time. At the level of the lowest frequency, $k = N$, the approximation is the product of the only scale coefficient at this level and scaling function corresponding to a base wavelet.

To be more specific, for the first two high-frequency levels, $k = 1$ and $k = 2$, the procedure of calculating the wavelet approximations contained the following operations:

$$\begin{gathered} a\ (i,1,2\cdot j-1) = s(i,2\cdot j) + s(i,2\cdot j-1)/2 \ \text{ for } \ j = 1:2^{N-1} \\ a(i,1,2\cdot j) = s(i,2\cdot j) + s(i,2\cdot j-1)/2 \ \text{ for } \ j = 1,2^{N-1} \\ a(i,2,4\cdot j-3) = a(i,1,4\cdot j) + a(i,1,2\cdot j)/2 \ \text{ for } \ j = 1:2^{N-2} \end{gathered} \tag{1}$$

$$a(i,2,4\cdot j-2)=a(i,1,4\cdot j)+a(i,1,2\cdot j)/2 \quad \text{for} \quad j=1:2^{N-2}$$

$$a(i,2,4\cdot j-1)=a(i,1,4\cdot j)+a(i,1,2\cdot j)/2 \quad \text{for} \quad j=1:2^{N-2}$$

$$a(i,2,4\cdot j)=a(i,1,4\cdot j)+a(i,1,2\cdot j)/2 \quad \text{for} \quad j=1:2^{N-2} \tag{2}$$

Recurrent calculations are continued in the analogous manner for level $k = N$.

Wavelet detail calculations at each level are performed by means of simple calculations of consecutive differences.

– at the first representation level of the highest frequency $k = 1$

$$d(\,i,1,j)=s(i,j)-a(i,1,j) \quad \text{for} \quad j\ =\ 1,2^N \tag{3}$$

– at the remaining levels $1 < k <= N$

$$d(\,i,k,j)=a(i,k-1,j)-a(i,k,j) \quad \text{for} \quad j=1,2^N \tag{4}$$

Appropriate wavelet coefficients are calculated using the fact that both the base wavelet and its equivalents at the consecutive representation levels, including wavelets shifted in time inside the wavelet carriers from levels of higher k value, corresponding with the details' shape, have unit energy.

$$wf(i,k,l)=\frac{d(i,1,j)}{2^{\frac{k-1}{2}}} \text{ for } l=1,2^{N-k};\ j=(l-1)\cdot 2^k+1,\ \ l\cdot 2^k \tag{5}$$

The condition of wavelet base normalisation is achieved by introducing the normalising coefficient $2^{\frac{k-1}{2}}$. In this manner, during the transition from the representation level k to level $k + 1$, the scaling of base elements occurs in a relationship, which equals the inverse square root.

The introduction of this coefficient causes a situation in which the orthonormal element standard of the basic set, as the integral from signal squared, on its support, has a unitary value. When the condition of normalisation is met, the measuring signal transformation into the representation, which is the sum of the consecutive details from level $k = 1$ to level $k = N$ and approximation at the level $k = N$, is a reversible transformation. It is worth noting that the details of the representation levels for each higher value k_1 are kept in the following approximations at levels with lower values $k < k_1$.

At each representation level, the detail is the sum of wavelet products shifted in time in relation to each other. These are shifted by the multiple of the value of their support and the appropriate wavelet coefficients, which have unit energy. Each wavelet shifted in time by the support value at the selected representation level corresponds to one wavelet coefficient. Both the number of those wavelets and the number of coefficients corresponding to them at level k equals 2^{N-k}.

Both the detail values and wavelet coefficient representation at each representation level [4] can be important indicators of the dynamic object condition. The detail energy and the energy distribution of wavelet coefficients are particularly important diagnostic

indicators. Knowledge of energy distribution of signal wavelet coefficients can show the directions of this signal's energy flow and fluctuations between frequency levels, which cannot be shown by the total detail energy in a given support. Using the calculated approximations at all representation levels, the scale coefficients can be calculated in a similar manner to details. Similar to wavelet coefficients and details, the sum of energy of each scale coefficient at the given representation level equals the wavelet approximation energy at that level. The distribution of scale coefficients and also the distribution of their energy is a complementary diagnostic indicator, which is sometimes used in the packet analysis process [5].

The multiresolution analysis of machine signal sampling applied in this paper with a frequency of 50 kHz was performed by means of discrete wavelet transform with the use of a simple analysing wavelet. In this analysis, specific frequency bands were assigned to each representation level, these are shown in Table 1.

Table 1

Detail frequency ranges of machine signal multiresolution analysis

Detail number	Frequency range [Hz]	Detail number	Frequency range [Hz]
D1	25 000–50 000	D7	390.625–781.25
D2	12 500–25 000	D8	195.3125–390.625
D3	6 250–12 500	D9	97.65625–195.3125
D4	3 125–6 250	D10	48.828125–97.65625
D5	1 562.5–3 125	D11	24.4140625–48.828125
D6	781.25–1 562.5	D12	12.20703125–24.4140625

4. Calculation of detail energy values in frequency bands of wavelet representation for the used diagnostic signals

One of the main indicators in signal diagnostics is stating the proportion of the energy of a selected element of multiresolution decomposition within the total energy of the diagnostic signal. The information about the absolute energy value calculated for various diagnostic signals used in analyses and carried by all decomposition details is also important. The results of such an analysis are shown in Table 2.

It can be observed that the best potential for the fault detection of short circuit type 1–2 and 1–3 can be achieved using voltage signal analyses proportional to the axial magnetic flux. Accurate results of this analysis are shown in Fig. 4–7. For the presentation, a support of length $2^{12} = 4096$ signal samples was chosen, starting from the consecutive sample No. 24576 and finishing with sample No. 28672 in the measuring files. The choice of the number of frequency levels of $N = 12$ was dictated by the use of the full sampling frequency while providing computational efficiency of a diagnostic system for use in real time.

Table 2

Absolute energy values of the detailed portion of wavelet representation for the diagnostic signals used in this paper

Measured signal detail energy		Chosen number of frequency levels for full representation *N*			
Signal	unit	12 – symmetrical motor	12 – short circuit 1–2	12 – short circuit 1–3	comment
phase L1current [$A^2 \cdot s$]		1048.55	1052.45	1063.25	increase
phase L2 current [$A^2 \cdot s$]		1064.31	1032.75	1090.54	
phase L3 current [$A^2 \cdot s$]		1078.90	1106.64	1092.75	increase
phase L1 voltage [$V^2 \cdot s$]		7 473 232	7 522 642	7 323 538	
phase L2 voltage [$V^2 \cdot s$]		7 400 333	7 385 624	7 264 234	decrease
phase L3 voltage [$V^2 \cdot s$]		7 514 143	5 554 712	7 366 448	
electromagnetic moment [$N^2m^2 \cdot s$]		56.6945	93.5757	33.2604	
signal ~ rotational speed [$V^2 \cdot s$]		814.357	810.495	796.257	
signal ~magnetic axial flux [$Wb^2 \cdot s$]		28.7314	31.3312	38.1515	increase
short circuit current [A^2]		0.0111	0.0831	0.2332	increase
vibration acceleration – axis X 1 [m^2/s^3]		0.0395	0.0326	0.0403	
vibration acceleration – axis X 2 [m^2/s^3]		0.0540	0.0363	0.0465	
sound pressure [$Pa^2 \cdot s$]		0.0141	0.0067	0.0101	
zero voltage [$V^2 \cdot s$]		18.6411	18.2989	17.662	decrease

As can be observed, the highest values of amplitudes are obtained for selected details of levels 9 and 10. At representation level 9, the signal representing a machine with a short-circuit type 1–2, is significantly dominant. A machine keeping a symmetrical supply has an amplitude, which is smaller by about 30%. At level 10, the detail of a machine with a short-circuit type 1–4, is dominant. A detail of machine with a short-circuit type 1–3 has an amplitude, which is smaller by about 25%. This is reflected in detail energy values at the representation levels shown in Fig. 7.

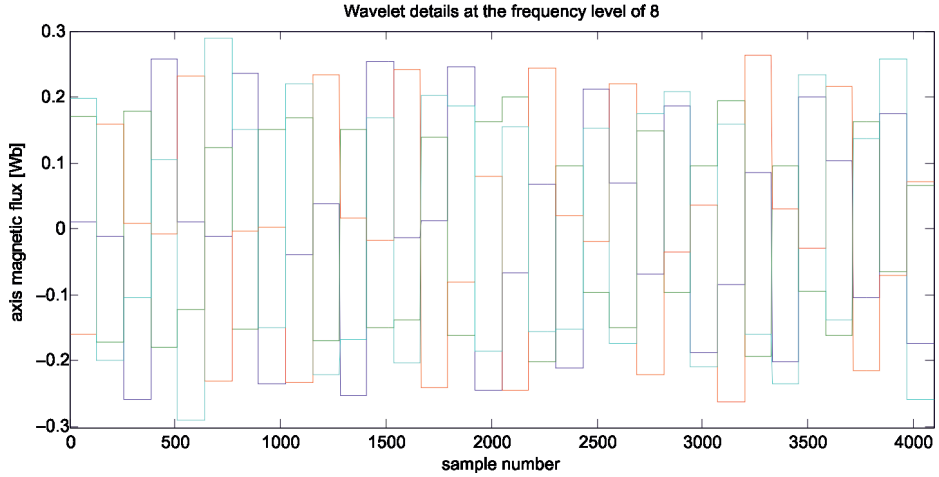

Fig. 4. Wavelet details of axial magnetic flux signal at the frequency level of 8 [D8 – colours: navy blue – symmetrical motor; green – short circuit 1–2; red – short circuit 1–3; blue – short circuit 1–4]

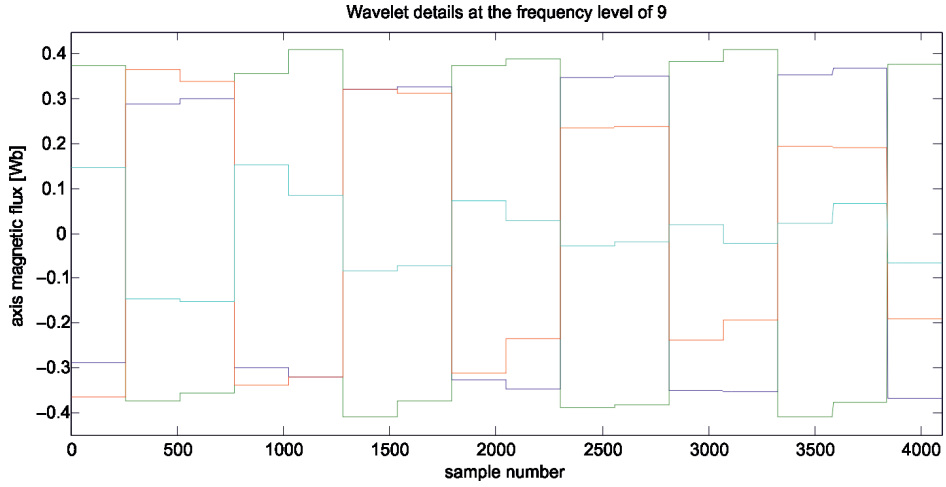

Fig. 5. Wavelet details of axial magnetic flux signal at the frequency level of 9 [D9 – colours: navy blue – symmetrical motor; green – short circuit 1–2; red – short circuit 1–3; blue – short circuit 1–4]

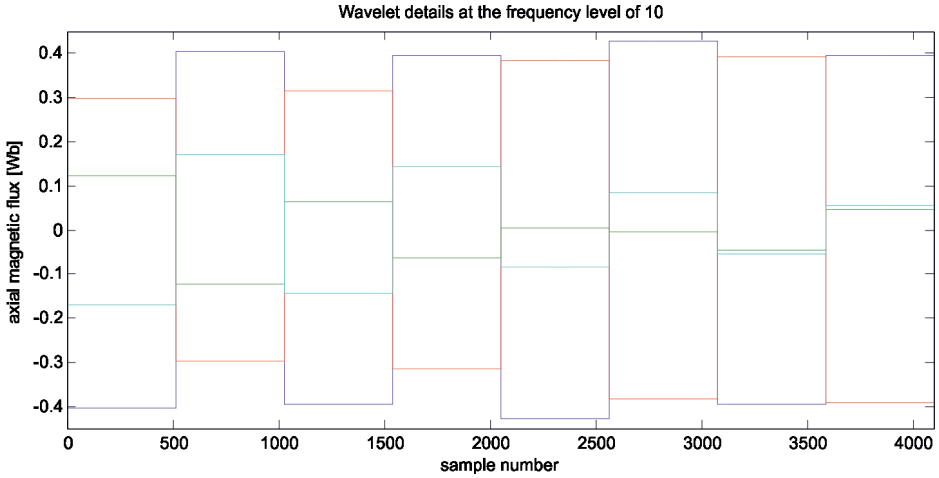

Fig. 6. Wavelet details of axial magnetic flux signal at the frequency level of 10 [D10 – colours: navy blue – symmetrical motor; green – short circuit 1–2; red – short circuit 1–3; blue – short circuit 1–4]

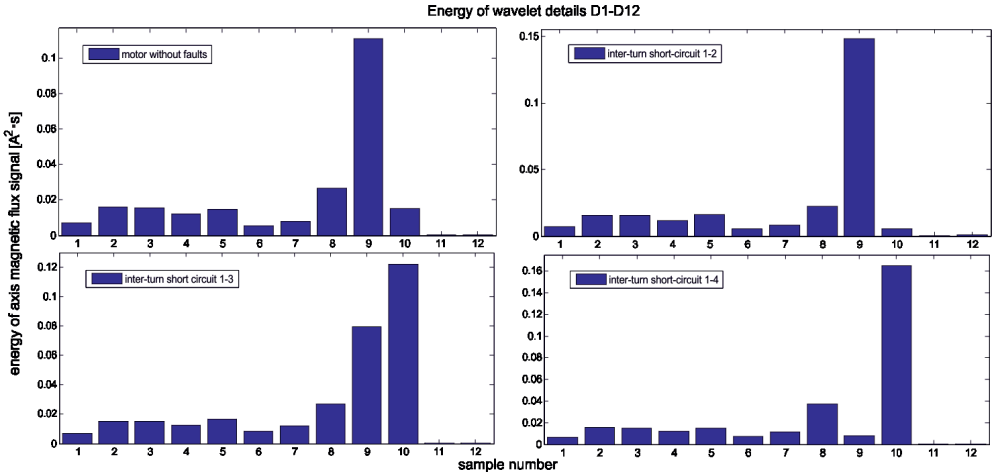

Fig. 7. Comparison of detail energy in the examined support from sample No. 24576 to sample No. 28672

Analyses performed across the entire measuring range over a duration of 10 seconds show that the detail energy of the signal proportional to axial magnetic flux in a stationary state, flows periodically between adjacent details, in this case, mainly between 9 and 10, keeping an approximately constant value of the sum of the energy of those details. As was stated during the analysis, the fluctuations take place with similar frequencies for both the machine with the symmetrical supply as well as the machine with faulty windings. This frequency is about 2 Hz. Whilst analysing the wavelet coefficients for the medium for samples from 24576 to 28672, shown in Fig. 8–11, it can be observed that there are current directions of those flows for symmetrical supply and three types of inter-turn short circuits.

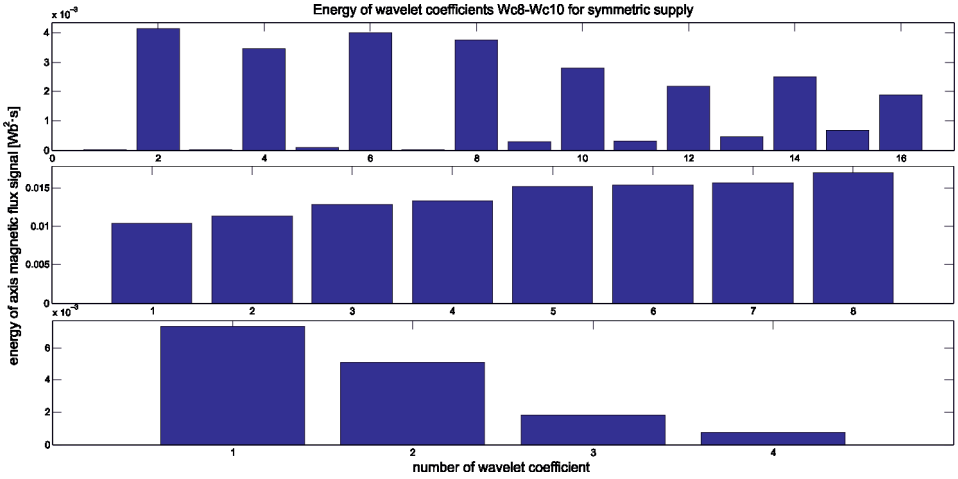

Fig. 8. Energy of wavelet coefficients of signal proportional to axial magnetic flux for the most important levels of wavelet representation from 8 to 10 – the case with symmetrical supply

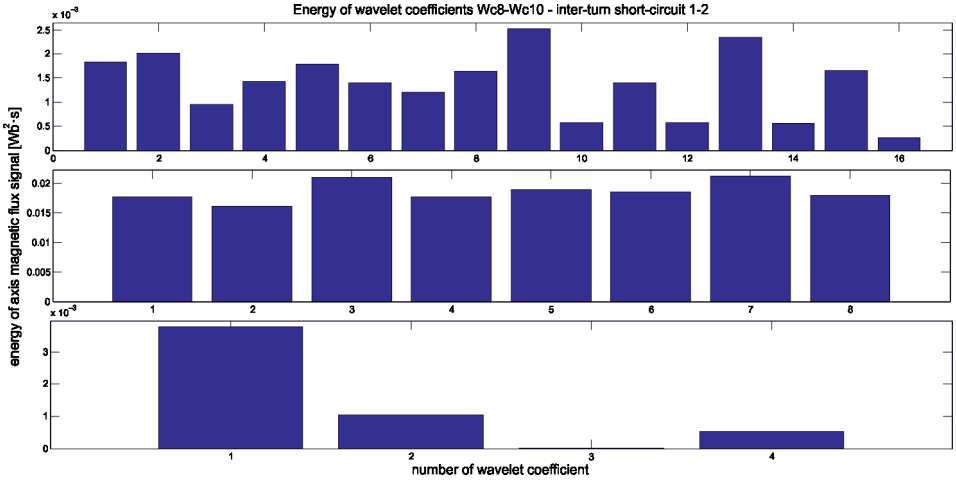

Fig. 9. Energy of wavelet coefficients of signal proportional to axial magnetic flux for the most important levels of wavelet representation from 8 to 10 – the case with the inter-turn short-circuit type 1–2

In the case of symmetrical supply in the support in which the analysis was performed, the energy of wavelet coefficients at the representation level 9 shows a steady increase and at level 10 a steady decrease. At level 8, whose coefficients values are less significant, the coefficients show a clear tendency to diverge in pairs.

As can be observed in Fig. 9, in the case of inter-turn short-circuit type 1–2, in the support, in which the analysis was performed, the energy of wavelet coefficients at the representation level 9 reached the maximum value at times of periodic flow. While the energy of wavelet coefficients at representation level 10 reached the minimum value.

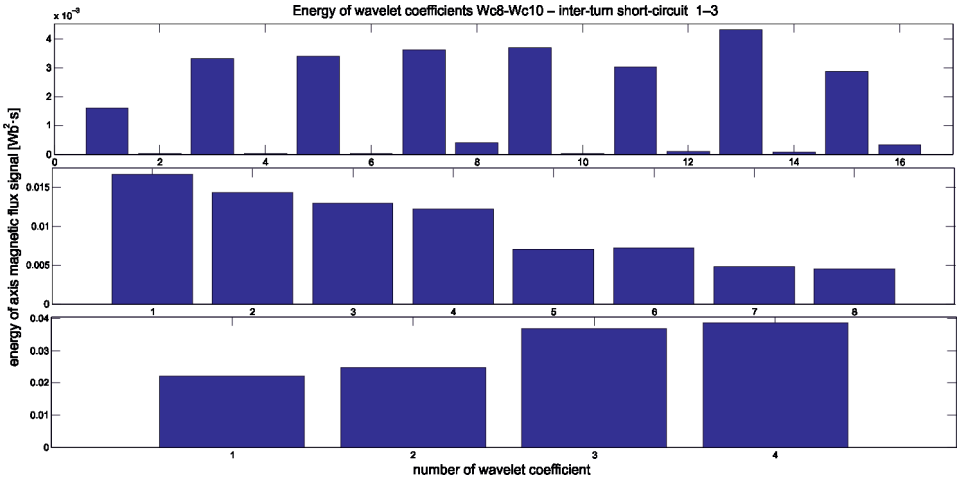

Fig. 10. Energy of wavelet coefficients of signal proportional to axial magnetic flux for the most important levels of wavelet representation from 8 to 10 – the case with inter-turn short-circuit type 1–3

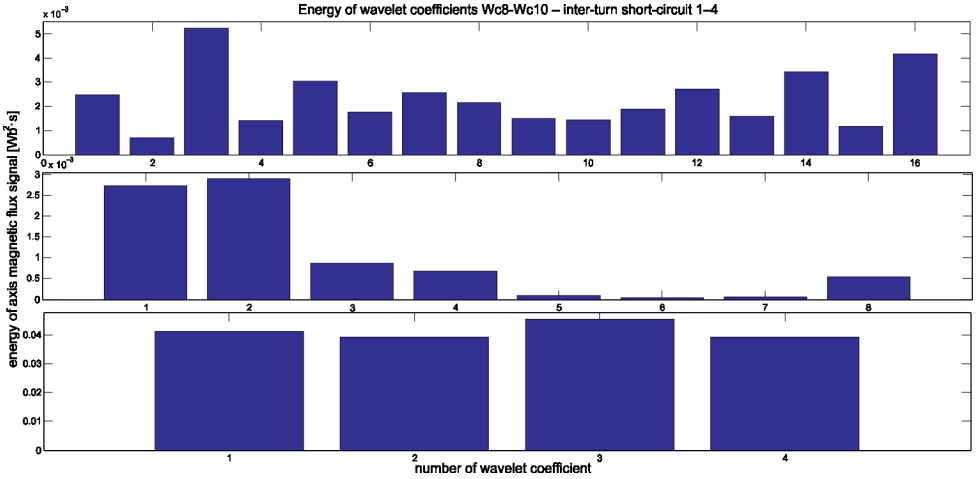

Fig. 11. Energy of wavelet coefficients of signal proportional to axial magnetic flux for the most important levels of wavelet representation from 8 to 10 – the case with inter-turn short-circuit type 1–4

In the case of a short circuit of windings 1–3 in the support in which the analysis was performed, there are opposite tendencies to those in the case of symmetrical supply. A steady decrease can be observed at representation level 9 and a steady increase can be observed at representation level 10. At level 8, whose coefficient values are less significant, every second coefficient has a significantly higher value than the coefficient before and after it.

In the case of inter-turn short-circuit type 1–4 in a support in which the analysis was performed the energy of wavelet coefficients at the representation level 9 reached the minimum value at times of periodic flow. While the energy of wavelet coefficients at representation level 10 reached the maximum value. The situation is opposite to the case presented in the analysis of the course of the voltage proportional to axial magnetic flux for short-circuit type 1–2. Both courses were measured during different experiments; thus, the described difference in energy states should be understood to be accidental. The comparison of energy distributions in a wider time range of 10 seconds with absolute energy values in the detailed part of wavelet representation shown in Table 2 allows for the statement that by using a signal proportional to axial flux, an effective detection can be performed, eliminating the effects of the described energy fluctuations between levels of the signal's wavelet coefficients. The very stable obtained result of the energy percentage distribution in wavelet details for a fault selected from all faults presented in Tables 2 and 3 constitutes a strong argument supporting this thesis. After passing through the initial 6–7 consecutive stages of calculations in which each stage analysis 2^{12} of consecutive samples from measuring files, the calculated energy percentage contribution for each detail does not change significantly. A similar remark can be made about absolute energy values of all details of multiresolution representation shown in Table 2. The average value of those details in one calculation cycle does not change significantly after calculating the first 6–7 calculation stages. Both of these remarks indirectly confirm that energy flows between levels are periodic functions with a mean value of zero.

Table 3

Energy percentage distribution in wavelet details at different representation levels

Frequency level	Energy percentage distribution among detailed elements of wavelet representation [%]			
	Symmetrical supply	Short-circuit 1–2	Short-circuit 1–3	Comments
1	3.0660	2.7559	2.2087	decrease
2	6.8091	6.1711	4.9120	decrease
3	6.6122	6.0019	4.8842	decrease
4	5.2402	4.7719	3.9185	decrease
5	6.3657	5.8252	4.9819	decrease
6	2.3528	2.1326	2.2771	
7	3.5622	3.4406	3.6229	
8	10.4763	10.9235	11.4012	increase
9	28.5709	30.1596	31.7637	increase
10	26.8059	27.6439	29.8805	increase
11	0.0482	0.0546	0.0415	
12	0.0903	0.1193	0.1079	

The absolute value of signal energy contained in a selected detail is the energy product contained in all representation details (Tab. 2) and in the detail percentage contribution at the selected level. For the three consecutive cases (machine symmetric supply, inter-turn short-circuit 1–2 and inter-turn short-circuit 1–3) both of these factors of the mentioned products, which correspond with one of the three cases are monotonic. For any number of

samples exceeding the number by 6–7 calculation stages, which means that for the number of samples equal to 2^{12} for each stage there are about 30 000 samples, the following inequality occurs:

$$E_d[i,sym,k] < E_d[i,1-2,k] < E_d[i,1-3,k] \text{ for } k = 9,10 \tag{6}$$

For the examined machine, after the analysis, the differences in the degree of difficulty of the correctly-performed diagnoses can be stated for two levels with the best selectiveness:

$$E_d[i,sym,k] < \Delta E_d[sym,1-2] = E_d[i,1-2,k] \text{ for } k = 9,10 \tag{7}$$

$$E_d[i,sym,k] < \Delta E_d[sym,1-3] = E_d[i,1-3,k] \text{ for } k = 9,10 \tag{8}$$

$$E_d[i,1-2,k] < \Delta E_d[1-2,1-3] = E_d[i,1-3,k] \text{ for } k = 9,10 \tag{9}$$

For measuring signals recorded with sampling frequency 50 kHz in time interval 10 seconds at level $k = 9$ they are approximately:

– $\Delta E_d(sym,1-2)$ 2.64 [Wb^2 · s],
– $\Delta E_d(sym,1-3)$ 11.68 [Wb^2 · s],
– $\Delta E_d(1-2,1-3)$ 6.93 [Wb^2 · s].

The obtained results of equations (7), (8) and (9) can be compared with total energy values of full detail representation shown in Table 2. In the case of machine symmetrical supply, inter-turn short-circuit 1–2 and inter-turn short-circuit 1–3, for the analyses of magnetic axial flux signal performed in the time interval 10 seconds, the differences are 28.73, 31.33 and 38.15 [Wb^2 · s] respectively. This comparison indicates that the presented method can be fully used in diagnostic practice.

5. Summary

The loaded squirrel-cage induction motor working in a steady state is a non-stationary dynamic object. Energy distributions of various signal types change their character over time. This fact significantly justifies the choice of a time and frequency method as a research tool.

The choice of the signal, which is going to be used in the analysis after recording, is a serious problem. After carrying out many tests, voltage signal proportional to magnetic axial flux was chosen. The axial flux is usually measured by means of a coil wound on a machine shaft and its Fourier spectrum was used in literature to detect faults, rotor eccentricity and also short-circuits in stator windings.

However, the detection of some faults whose effect is tiny even in a steady state, at constant load, still constitutes a difficult task especially because of the overlapping of non-stationary fluctuations of variables carrying energy connected with an alternating magnetic field and also because of various types of interference during measurement.

The analyses in the time and frequency domain with the use of the simple wavelet base, based on the application of orthogonal Walsh and Haar functions, allowed the generation of full multiresolution representation for all examined measuring signals, also phase currents and voltages. In this case, those parts of courses, which were visibly distorted, were mainly

analysed; however, the results, which have been obtained so far, are less useful in diagnostics in comparison to the analyses of axial flux signal presented in this paper.

It should be emphasised that the applied methodology of the calculation of detailed elements of full time and frequency representation presented in this paper, simple as it seems, can be used in a laboratory measuring system without the need to acquire specialist software.

Acknowledgment

Presented results of the research, which was carried out under the themes No. E-2/581/2016/DS, No. E-3/627/2016/DS were founded by the subsidies on science granded by Polish Ministry of Science and Higher Education.

References

[1] Assaf T., Henao H., Capolino G.A., *Simplified axial flux spectrum method to detect incipient stator inter-turn short-circuits in induction machine*, 2004 IEEE International Symposium on Industrial Electronics, ISIE, Ajaccio, vol. 2, 4–7 May 2004, 815–819.

[2] Antal M., Antal M., *Zwarcia zwojowe w uzwojeniu stojana klatkowego silnika indukcyjnego*, Prace Naukowe Instytutu Maszyn, Napędów i Pomiarów Elektrycznych, Nr 59, Politechnika Wrocławska, Studia i materiały, Nr 26, 2006, 78–88.

[3] Antal M., Antal L., Zawilak J., *Badania uszkodzeń uzwojenia stojana klatkowego silnika indukcyjnego*, Zeszyty Problemowe – Maszyny Elektryczne, Nr 76, 2007, 83–88.

[4] Zając M., Sułowicz M., *Wavelet Detectors for Extraction of Characteristic Features of Induction Motor Rotor Faults*, International Conference on Signals and Electronic Systems, ICSES 2016, 4–7 Sept., Kraków 2016.

[5] Glabisz W., *State analysis of time-varying linear systems via Walsh-wavelets packets*, Archives of Civil and Mechanical Engineering, No. 3, 2003, 59–75.

[6] Asfani D.A., Muhammad A.K., Syafaruddin, Purnomo M.H., Hiyama T., *Temporary short circuit detection in induction motor winding using combination of wavelet transform and neural network*, Expert Systems with Applications, vol. 39, Issue 5, April 2012, 5367–5375.

[7] Głowacz A., *Diagnostics of direct current machine based on analysis of acoustic signals with the use of symlet wavelet transform and modified classifier based on word*s. Eksploatacja i Niezawodność – Maintenance and Reliability, 2014, Vol. 16, no. 4, 554–558.

[8] Wolkiewicz M., Tarchała G., Orłowska-Kowalska T., Kowalski C. T., *Online Stator Interturn Short Circuits Monitoring in the DFOC Induction-Motor Drive*, IEEE Transactions on Industrial Electronics, vol. 63, no. 4, April 2016, 2517–2528.

[9] Ogidi O.O., Barendse B.S., Khan M.A., *The Detection of Interturn Short Circuit Faults in Axial-Flux Permanent Magnet Machine with Concentrated Windings*, 2015 IEEE Energy Conversion Congress and Exposition, September 2015, 1810–1817.

[10] Pietrowski W., *Wavelet Analysis of Current of an Induction Machine with Time-Varied Short Circuit*, Proceedings of XXIII Symposium Electromagnetic Phenomena in Nonlinear Circuits, 2–4 July 2014, Pilsen, Czech Republic, 179–180.
[11] Pietrowski W., *Wavelet analysis of axial flux in an induction machine on no-load test*, Przegląd Elektrotechniczny, Vol, 7b/2012, 20–23.
[12] Bessam B., Menacer A., Boumehraz M., Cherif H., *Wavelet transform and neural network techniques for inter-turn short circuit diagnosis and location in induction motor*, Int Journal of System Assurance Engineering Management, 2015, 1–11.
[13] Lai C., Balamurali A., Bousaba V., Iyer K.L.V., Kar N.C., *Analysis of stator winding inter-turn short-circuit fault in interior and surface mounted permanent magnet traction machines*, Proceeding of IEEE ITEC'14, 2014, 1–6.